The Astrophysical Journal, 743:132 (9pp), 2011 December 20 doi:10.1088/0004-637X/743/2/132

SPECTROSCOPIC CONFIRMATION OF $z \sim 7$ LYMAN BREAK GALAXIES: PROBING THE EARLIEST GALAXIES AND THE EPOCH OF REIONIZATION

L. Pentericci[1], A. Fontana[1], E. Vanzella[2], M. Castellano[1], A. Grazian[1], M. Dijkstra[3], K. Boutsia[1], S. Cristiani[2], M. Dickinson[4], E. Giallongo[1], M. Giavalisco[5], R. Maiolino[1], A. Moorwood[6,7], D. Paris[1], and P. Santini[1]
[1] INAF Osservatorio Astronomico di Roma, Via Frascati 33,00040 Monteporzio (RM), Italy; laura.pentericci@oa-roma.inaf.it
[2] INAF Osservatorio Astronomico di Trieste, Via G. B. Tiepolo 11, 34131 Trieste, Italy
[3] Max-Planck-Institut für Astrophysik, Karl-Schwarzschild-Str. 1, 85741 Garching, Germany
[4] National Optical Astronomy Observatory, P.O. Box 26732, Tucson, AZ 85726, USA
[5] Department of Astronomy, University of Massachusetts, 710 North Pleasant Street, Amherst, MA 01003, USA
[6] European Southern Observatory, Karl-Schwarzschild Strasse, 85748 Garching bei Munchen, Germany
Received 2011 July 7; accepted 2011 August 31; published 2011 November 30

ABSTRACT

We present the final results from our ultra-deep spectroscopic campaign with FORS2 at the ESO Very Large Telescope (VLT) for the confirmation of $z \simeq 7$ "z-band dropout" candidates selected from our VLT/Hawk-I imaging survey over three independent fields. In particular, we report on two newly discovered galaxies at redshift ∼6.7 in the New Technology Telescope Deep Field. Both galaxies show an Lyα emission line with rest-frame equivalent widths (EWs) of the order of 15–20 Å and luminosities of (2–4) $\times 10^{42}$ erg s^{-1}. We also present the results of ultra-deep observations of a sample of i-dropout galaxies, from which we set a solid upper limit on the fraction of interlopers. Out of the 20 z-dropouts observed we confirm 5 galaxies at $6.6 < z < 7.1$. This is systematically below the expectations drawn on the basis of lower redshift observations: in particular, there is a significant lack of objects with intermediate Lyα EWs (between 20 and 55 Å). We conclude that the observed trend for the rising fraction of Lyα emission in Lyman break galaxies from $z \sim 3$ to $z \sim 6$ is most probably reversed from $z \sim 6$ to $z \sim 7$. Explaining the observed rapid change in the Lyα emitter fraction among the dropout population with reionization requires a fast evolution of the neutral fraction of hydrogen in the universe. Assuming that the universe is completely ionized at $z = 6$ and adopting a set of semi-analytical models, we find that our data require a change of the neutral hydrogen fraction of the order of $\Delta\chi_{\rm H\,I} \sim 0.6$ in a time $\Delta z \sim 1$, provided that the escape fraction does not increase dramatically over the same redshift interval.

Key words: galaxies: distances and redshifts – galaxies: formation

Online-only material: color figures

1. INTRODUCTION

The epoch of reionization marks a major phase transition of the universe, during which the intergalactic space became transparent to UV photons. Determining when this occurred and the physical processes involved represents the latest frontier in observational cosmology. Over the last few years, searches have intensified to identify the population of high-redshift galaxies that might be responsible for this process. Recent data from the *Hubble Space Telescope* WFC3 infrared camera provided a dramatic advance accessing the faint side of the $z \sim 7$ UV luminosity function (LF; McLure et al. 2010; Bouwens et al. 2010a; Grazian et al. 2011), while wide-field ground-based surveys are starting to detect the brightest galaxies at $z \sim 7$ (Ouchi et al. 2009; Castellano et al. 2010a, 2010b, C10a, C10b from here on). These surveys provided evidence that the UV LF evolves significantly with redshift (Wilkins et al. 2010), that the UV continuum of galaxies appears progressively bluer with increasing z (Finkelstein et al. 2010; Bouwens et al. 2010b, but see also Dunlop et al. 2011), and that their stellar masses are on average smaller than those of their lower-z counterparts (Labbé et al. 2010), while the morphologies remain essentially unchanged from $z \sim 6$ to $z \sim 7$ (Oesch et al. 2010).

Unfortunately, these results are entirely based on color-selected samples without spectroscopic confirmation. The lack of spectroscopic redshifts prevents us from deriving firm conclusions based on these early samples. First, an unknown fraction of interlopers biases the estimates of size and redshift distribution which are needed to compute the LF. The lack of spectroscopic redshifts also introduces degeneracies in the spectral energy distribution (SED) fitting that make the masses and other physical properties poorly determined.

Finally, only spectroscopic observations of high-z Lyα emission have the potential to provide a definitive answer to the major question of how and when reionization occurred (Dayal et al. 2011; Dijkstra et al. 2011). The Lyα emission line is a powerful diagnostic since it is easily erased by neutral gas outside galaxies. Its observed strength in distant galaxies is therefore a sensitive probe of the latest time when reionization was completed (e.g., Robertson & Ellis 2011). Indeed, some recent studies pointed to a decrease in the number of Lyα emitters (LAEs) at $z \sim 7$ (Ota et al. 2010) and failed to detect bright LAEs at even higher redshift (Hibon et al. 2010). In a recent work, we also found a significant lack of intense Lyα in ultra-deep spectra of candidate $z \sim 7$ Lyman break galaxies (LBGs; Fontana et al. 2010, F10 from here on). All these works seem to indicate that we might be approaching the epoch when the intergalactic medium (IGM) was increasingly neutral.

[7] We would like to dedicate this paper in memory of Alan Moorwood, who left us a few days before the paper was submitted. Alan was fundamental to the development of Hawk-I, which enabled this survey and many other important observing programs. He had clear foresight of the instrument's impact on the search for the highest redshift galaxies. More importantly, he always urged us to obtain spectroscopic confirmation of the candidates and was eagerly awaiting the results of this effort.

To address these issues, we have carried out a systematic follow-up of our sample of $z \sim 7$ candidates. Galaxies were initially selected as z-dropouts in three independent fields, the GOODS-South field (Giavalisco et al. 2004), the New Technology Telescope Deep Field (NTTDF; Arnouts et al. 1999; Fontana et al. 2000), and the BDF-4 field (Lehnert & Bremer 2003) from deep near-IR Hawk-I observations, covering a total area of 200 arcmin^2, complemented by WFC3 observations (C10a; C10b). We then carried out deep spectroscopic observations with FORS2. The first results were published in F10 where we reported the confirmation of a weak Lyα emission line at $z = 6.97$ in the GOODS-South field, and in Vanzella et al. 2011 (V11 from here on) where we presented two galaxies in the BDF-4 field, showing bright Lyα emission at $z \approx 7.1$.

In this final paper, we present the results on the z-dropouts obtained in the NTTDF, where we confirm two further galaxies at $z \geqslant 6.6$ through the presence of Lyα emission. We also present and briefly discuss the results obtained on the i-dropout galaxies that were observed in the three separate fields as secondary targets.

Finally, we give an overview of the results obtained in the entire z-dropout sample and compare them to the expectations based on lower redshift observations to determine the redshift evolution of the fraction of LAEs in LBG samples. We discuss the implications of our results on the epoch of reionization.

All magnitudes are in the AB system, and we adopt $H_0 = 70$ km s^{-1} Mpc^{-1}, $\Omega_M = 0.3$, and $\Omega_\Lambda = 0.7$.

2. NTTDF TARGET SELECTION AND OBSERVATIONS

The targets were selected as candidate $z \sim 7$ galaxies according to the criteria described extensively in C10b: besides the five z-band dropout candidates listed in Table 3 of that paper, two further z-band dropouts were also included in the slits. These two objects (NTTDF–474 and NTTDF–2916) have Y-band magnitudes that are slightly fainter than the completeness limit applied in C10b to derive the LF (they have, respectively, $Y = 26.53$ and $Y = 26.67$) but otherwise their photometry is entirely consistent with the z-dropouts selection. In the remaining slits, we placed several i-dropout candidates (see Section 3.2) and other interesting objects such as a few of the interlopers described in C10a, which will be discussed in a future paper.

Observations were taken in service mode with the FORS2 spectrograph on the ESO Very Large Telescope, during 2010 July–August. We used the 600Z holographic grating that provides the highest sensitivity in the range 8000–10000 Å with a spectral resolution $R \simeq 1390$ and a sampling of 1.6 Å pixel^{-1} for a 1″ slit. The data presented here come from the co-addition of 86 spectra of 665 s of integration each, on a single mask, for a total of 57120 s (15.9 hr), with median seeing around 0.″8. The sources have been observed through slitlets 1″ wide by 12″ long. Series of spectra were taken at two different positions, offset by 4″ (16 pixels) in the direction perpendicular to the dispersion.

Standard flat-fielding, bias subtraction, and wavelength calibration have been applied as in Vanzella et al. (2009, 2011) and F10. The sky background has been subtracted between consecutive exposures, exploiting the fact that the target spectrum is offset due to dithering. Before combining frames, particular care has been devoted to the possible offset along the wavelength direction, by measuring the centroids of the sky lines in the wavelength interval 9400–9900 Å. We have also carried out the sky subtraction by fitting a polynomial function to the background. The two approaches provide consistent results.

Finally, spectra were flux-calibrated using the observations of spectrophotometric standards. Based on the analysis of the standard star observed with the same setup of science targets, we derive that the relative error due to flux calibration is less than 10%. We expect slit losses to be small, given the extremely compact size of the targets (none of the spectra appear to be resolved along the spatial direction) and the excellent seeing during the observations and therefore we neglect them in the subsequent discussion.

We note that we used exactly the same setup and integration times as in the previous observations, presented in F10 and V11. The reduction and calibration procedures employed were also the same: this implies that we have a very homogeneous set of observations and that the spectra have a uniform final depth.

3. RESULTS

3.1. Observations of z-dropouts

In Table 1, we present the results for all the z-dropouts observed in the NTTDF. The galaxies observed in the GOODS field were already discussed in F10. We also discuss the z-dropouts in the BDF-4 field that were observed but not spectroscopically confirmed (the two LAEs at $z > 7$ in this field were extensively described in V11). We discuss all sources where some feature is detected and the possible identification(s).

NTTDF–474. This object shows a faint line at 9270 Å and no continuum in agreement with the faint broadband magnitude. We exclude an identification with one of the [O II] components since we would see the other component as well (the line falls on an area that is free from sky lines) and given our resolution (see also the discussion in V11). We also exclude an identification with one of the two [O III] components or Hβ: in these cases we would simultaneously detect the three lines (at 5007, 4959, and 4861 Å, respectively) which all fall in sky-free portions of the spectrum. Finally, if the line were Hα from a low-redshift object, then the large drop observed between the z and Y band of more than 1.6 mag, as well as the non-detections in the V, R, and I band down to AB = 29, would not be consistent with the redshift. We therefore conclude that the most likely identification is Lyα at $z = 6.623$. This redshift is in excellent agreement with the photo-$z = 6.8$. The final extracted one-dimensional and two-dimensional spectra of this object are presented in Figure 1. Note that the line shows no clear asymmetry, but given the low signal-to-noise ratio (S/N) we cannot make any firm conclusions based on this.

NTTDF–1917. This object shows an emission line at 8415 Å with flux 3.2×10^{-18} erg s^{-1} cm^{-2} and S/N ~ 9. In the same slit, we observe another emission line at 8640 Å: this line is much more diffuse (spatially) and has an offset along the spatial axis of ∼2–3 pixels corresponding to 0.″7. The offset is consistent with the position of a closeby diffuse galaxy. We believe that this second line is associated with the nearby object, whose light enters the slit. The two-dimensional spectrum is presented in Figure 2.

The line at 8415 Å cannot be identified with [O II] because we do not observe the typical double component. An identification with [O III] at $z = 0.68$ (either of the components) is also quite unlikely since the other [O III] component and Hβ should be visible in the spectra. In the case of identification with Hβ at $z = 0.73$, the [O III] component 5007 would fall on the top of a skyline so we could possibly fail to observe it. Finally for Hα at $z = 0.28$, the implied rest-frame equivalent width (EW) would

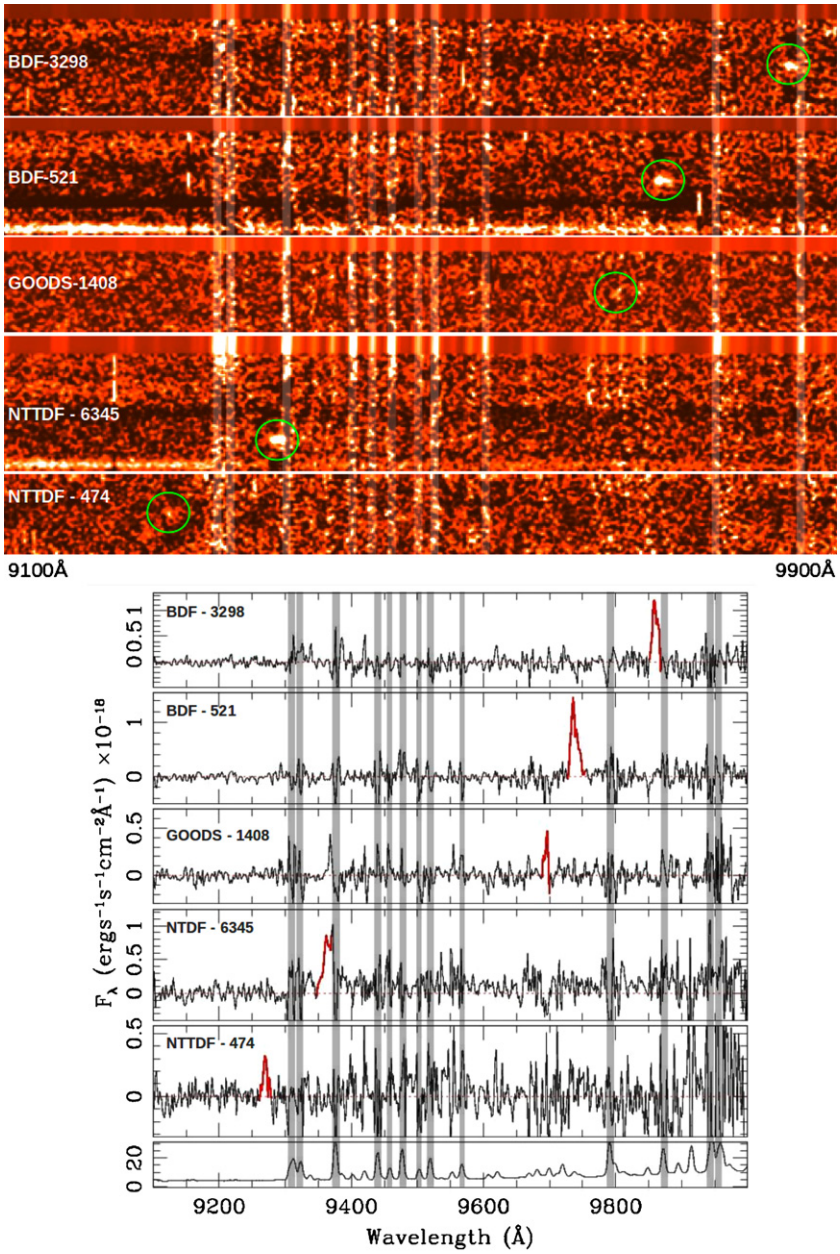

Figure 1. Top panel: the two-dimensional spectra of the five confirmed galaxies. The spectra have been filtered with the FILTER/ADAPTIV Midas task using a box of 3 × 3 pixels. Bottom panel: the extracted one-dimensional spectra of the five confirmed galaxies and of the sky. The bands indicate the positions of the strongest skylines that produce residuals in the reduced spectra.

(A color version of this figure is available in the online journal.)

Table 1
Spectroscopic Properties of Observed z-dropouts in the NTTDF and BDF-4 Fields

ID	R.A.	Decl.	Y	Feature	Identification	Flux (erg s^{-1} cm^{-2})	S/N
NTTDF–474	181.373976	−7.664256	26.50 ± 0.20	Line@9270 Å	Lyα@z = 6.623	3.2 × 10^{-18}	7
NTTDF–1479	181.342892	−7.681269	26.12 ± 0.13	No feature			
NTTDF–1632	181.385721	−7.683538	26.44 ± 0.18	No feature			
NTTDF–1917	181.321143	−7.687666	26.32 ± 0.15	Line@8415 Å	Lyα/Hβ	3.2 × 10^{-18}	9
NTTDF–2916	181.308925	−7.702437	26.64 ± 0.21	No feature			
NTTDF–6345	181.403901	−7.756190	25.46 ± 0.07	Line@9364.5 Å	Lyα@z = 6.701	7.2 × 10^{-18}	11
NTTDF–6543	181.383383	−7.759527	25.75 ± 0.09	Line@9566(tentative)	Associated with another object		
BDF4–2687	337.045197	−35.155960	26.15 ± 0.13	No feature			
BDF4–2883	337.028137	−35.160046	25.96 ± 0.11	No feature			
BDF4–5583	337.047363	−35.204590	26.65 ± 0.21	No feature			
BDF4–5665	337.051147	−35.205826	26.64 ± 0.20	No feature			

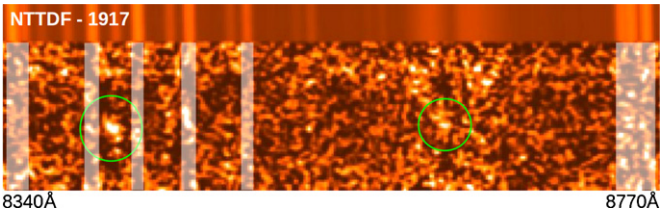

Figure 2. Two-dimensional spectrum of the contaminant galaxy NTTDF–1917 at a probable redshift 5.92. The bands indicate the positions of the strongest sky lines that produce residuals in the reduced spectra.

(A color version of this figure is available in the online journal.)

be unusually high (>300 Å): the shape of the SED also disfavors this option, given the non-detections in the *V*, *R*, and *I* band.

However, even the identification of the line as an Lyα emission poses some problems: the implied redshift of $z = 5.92$ is hardly compatible with the z-dropout selection function (see the redshift distribution in C10b). Indeed the best-fit z-phot solution is at 6.87, mainly based on the large color term $z - Y$. The fit is, however, still acceptable (reduced χ^2 2.0) also for the solution at $z = 5.92$, although the object would have to be a very young, dusty galaxy with an unusually high star formation rate (SFR), respectively, $E(B-V) = 0.25$ and SFR $= 170\ M_{\odot}\ \mathrm{yr}^{-1}$, adopting a Small Magellanic Cloud extinction law, which is appropriate for very young sources.

For the rest of the paper, we will consider this object as an interloper of the $z \sim 7$ sample.

NTTDF–6345. This objects shows a line at 9364 Å with flux 7.7×10^{-18} erg s^{-1} cm^{-2}. The flux estimate is actually somewhat uncertain due to two problems: the line falls quite close to a bright skyline (so the contribution of the red wing might have been poorly estimated) and there is a bright object 4″ away from our Galaxy that falls in the slit. The distance is exactly the same as our dither patter: as a result the zero flux level has some uncertainty. For the identification of the emission line, we follow the same consideration as for NTT–474 to exclude the lower redshift interpretation. Note that despite the vicinity of the skyline, we exclude the possibility that the emission line might be [O II] because the second component should be clearly visible 2 pixels outside the skyline. We conclude that the line is Lyα emission at redshift 6.701, in excellent agreement with the photometric redshift of 6.73. The extracted one-dimensional and the two-dimensional spectra of this object are presented in Figure 1.

NTTDF–6543. In the spectrum of this object, we tentatively detect an emission line falling exactly on the top of a skyline at λ9566. However, the emission is extremely faint, at the very limit of our detection sensitivity: in addition, there is a significant offset between its spatial position and the expected position of our target along the slit (approximately 3 pixels, 0.″75). Given the high uncertainty both in the reality of the line and in its association with the z-dropout candidate, we will consider this object as unconfirmed. Note that the inclusion of this object as a confirmed $z \sim 7$ galaxy would not affect any of the statistics on the Lyα fractions derived later in the paper, since its EW would be extremely low (given its faint line flux and relatively bright continuum magnitude).

3.2. Observations of *i*-dropouts

As mentioned in Section 2, some of the slits which were not filled with primary z-dropout candidates were used to observe candidate $z \sim 6$ galaxies. This was done also for the previous observations of the GOODS-South and BDF fields, and we report all results here. The *i*-dropouts were selected according to the following color criteria: for the GOODS-S field the selection is the same as in V10, namely $(i_{775} - z_{850}) > 1.3$ and $\mathrm{S/N}(B_{435}) < 2$ and $\mathrm{S/N}(V_{606}) < 2$; for the BDF and NTT fields the selection was $I - Z > 1.3$ and $\mathrm{S/N} < 2$ in all band blueward of the *I* band. We note again here that our initial catalog was *Y*-selected, therefore all objects were initially detected in the *Y* band with a limit of AB $\leqslant 27$ (C10a).

In Table 2, we report the results for all *i*-dropouts that were observed in the three independent fields. We report the line fluxes, total z-band magnitude, and the EW of the lines, after taking out the contribution of the line itself to the broadband magnitude for $z > 5.8$. The quality flags (A, B, and C) are set according to V09. We remark that these are among the deepest observations ever made on $z \sim 6$ galaxies, since typically all other studies employ much shorter integration times (4–8 hr, see, e.g., V10; Stanway et al. 2007). In total, 17 *i*-dropouts were observed: we determine an unambiguous redshift for 15 of the candidates, of which 14 are at redshift between 5.5 and 6.2 and 1 is an [O II] emitter at $z = 1.335$. Of the remaining two, one has no feature detected and in one we see faint continuum over most of the spectral range but we observe no break: moreover, this continuum is extremely extended spatially (more than 15 pixels), and hence its identification as a high-redshift object is highly dubious.

The immediate conclusion that we can draw from these observations is that the *i*-dropout selection is indeed very robust and that most of the objects that usually remain undetected in the medium-deep spectroscopic follow-up are indeed at redshift ∼6. We can set a very robust upper limit for the interloper fraction as ⩽18% (3/17; in the worst case where the uncertain object and the undetected one are both interlopers). We also note that the fraction of galaxies with Lyα in emission is actually quite high: 11 candidates show an Lyα line in emission, although often with small EWs.

4. REDSHIFT EVOLUTION OF THE Lyα FRACTION

4.1. Total Sample

In our spectroscopic campaign, we have observed 20 z-dropout candidates: in total, seven were observed in the GOODS-S field (F10) of which one was confirmed, six were observed in the BDF of which two were confirmed (V11), and finally seven were observed in the NTTDF of which two were confirmed (this paper). In Table 3, we report the basic properties of the five confirmed galaxies at $z > 6.5$, and in Figure 1 we show their one-dimensional and two-dimensional spectra. The EWs were calculated from the Lyα flux determined from the spectra and the continuum determined from the *Y*-band photometry. When appropriate, we corrected the *Y*-band flux from the Lyα contribution, which is subtracted, and for the IGM absorption which affects the *Y*-band filter (in practice, this is necessary only for the two objects at $z > 7$). The uncertainties on the EWs, derived from the flux calibration uncertainty and the photometric errors, are also reported. Only two of the confirmed galaxies have relatively bright Lyα emission and would also be selected as LAEs in narrowband surveys, given that their EW > 20 Å.

Overall we have confirmed 5 galaxies at $6.6 < z < 7.1$ out of the initial 20 objects observed. Of the remaining 15, object NTTDF–1917 is an interloper (although its redshift is uncertain) and 14 are undetected. The redshift distribution of the five

Table 2
Spectroscopic Properties of Observed *i*-dropouts

ID	R.A.	Decl.	z_{AB}	Feature	Ident.	Redshift	Flux (erg s^{-1} cm^{-2})	EW (Å)	Quality
NTT–1806	181.365212	−7.685984	26.81	Doublet@8709	[O II]	1.335			B
NTT–4025	181.331168	−7.718568	26.51	Line@8072	Lyα	5.638	1.6×10^{-18}	7	B
NTT–2313	181.380362	−7.693486	26.16	Continuum+break at 8550		6.07	...		B
NTT–7173	181.351769	−7.767678	26.73	Line@8474	Lyα	5.969	3.2	18	B
NTT–7246	181.380139	−7.770059	26.02	Line@8175+continuum	Lyα	5.724	4.24	12	A
BDF–2203	336.957961	−35.14716	26.39	Line@8656+continuum	Lyα	6.118	2.5	9.9	A
BDF–3367	336.956062	−35.167719	25.87	Continuum+break		5.73	...		B
BDF–4085	336.957328	−35.181049	26.13	Line@8750+continuum	Lyα	6.196	23.5	110	A
BDF–4568	336.960484	−35.188689	26.46	Faint diffuse continuum		low-z	...		C
BDF–5870	336.955504	−35.208964	26.67	Line@8064+continuum	Lyα	5.632	1.8	10	A
BDF–3995	336.979035	−35.179460	26.28	Line@8752+continuum	Lyα	6.198	2.1	7.3	A
BDF–2890	336.991181	−35.160187	25.51	Continuum+break at 8150		5.70	...		C
BDF–5889	336.998416	−35.209229	26.59	Line@7953 Å	Lyα	5.540	2.0	9.8	B
GOODSS–15052	53.145019	−27.762773	26.58	Line@8442 Å	Lyα	5.942	3.0	14	B
GOODSS–79	53.122540	−27.7605000	26.56	Line@8424 Å	Lyα	5.928	3.65	16	A
GOODSS–12636	53.151438	−27.720971	26.70	Line@8426 Å	Lyα	5.929	7.15	45	A
GOODSS–48	53.159500	−27.7714443	26.47	No feature			...		

Table 3
Spectroscopic Properties of Confirmed $z \sim 7$ Galaxies

ID	z	$L_{Ly\alpha}$ (erg s^{-1})	EW (Å)	S/N
BDF–3299	7.109	6.1×10^{42}	50 ± 10	16
BDF–521	7.008	7.1×10^{42}	64 ± 10	18
GOODS–1408	6.972	2.0×10^{42}	13 ± 5	7
NTTDF–6345	6.701	4.4×10^{42}	15 ± 3	11
NTTDF–474	6.623	1.7×10^{42}	16 ± 5	7

confirmed galaxies is in agreement with the one expected from the color selection criteria and derived in C10a. The obvious question to raise now is whether this rate of spectroscopic confirmation and the general modest EWs of the Lyα lines are in agreement with what was expected on the basis of lower redshift surveys of LBGs.

In the most recent and complete work on $z \sim 6$ galaxies, Stark et al. (2011, S11 from here on) found a very high fraction of LAEs among LBGs. They assembled a sample of 74 spectroscopically observed $z \sim 6$ galaxies by putting together their own Keck observations with all previous data available in the literature (e.g., V09; Dow-Hygelund et al. 2007; Stanway et al. 2004; Bunker et al. 2003). With this, they were able to confirm the redshift dependence of the fraction of line emission in LBGs, more robustly and to higher redshift than was possible before (e.g., Stanway et al. 2007; Vanzella et al. 2009). In particular, they found that 54% of faint ($M_{UV} > -20.25$) $z \sim 6$ LBGs show relatively strong (EW > 25 Å) emission and that a significant fraction (27%) has EW > 55 Å. For more luminous galaxies ($M_{UV} < -20.25$) the fractions are lower, but still about 20% of them are detectable as LAEs. Moreover, by comparing these numbers to analogous samples of LBGs at $z \sim 4$ and 5, they determined that there is a strong increase of the Lyα emission fraction with redshift. In particular, the evolution is very significant for the intermediate EW values with $dF^{25}_{Ly\alpha}/dz = 0.11 \pm 0.04$, where $F^{25}_{Ly\alpha}$ is the fraction of LBGs with Lyα stronger than 25 Å (in the original paper $\chi^{25}_{Ly\alpha}$) both for faint and bright galaxies. The increase is somewhat less pronounced for the brightest emitters with EW > 55 Å (Stark et al. 2011).

Their results suggest that, if the rise in the fraction of LBGs that show prominent Lyα emission observed over the epoch $4 < z < 6$ continues to $z \sim 7$, Lyα emission should be visible in many $z \sim 7$ galaxies.

It is therefore interesting to make a comparison between the observed distribution of Lyα emission in our sample and both the $z \sim 6$ observations by S11 and their predictions for $z \sim 7$. For this comparison, we will assume that all of our photometrically selected dropouts are genuinely at $z \sim 7$, even if we failed to confirm them spectroscopically. The exception is the object NTTDF–1917 that will be considered an interloper from here on and will be excluded from the sample. This is the same assumption made by S11, who found negligible contamination for luminous galaxies ($-22 < M_{UV} < -20$) which also make up the large majority of our sample, rising to only 10% for less luminous sources.

In Figure 3, we plot the results of S11 together with their predictions for $z = 7$, which were derived by fitting a linear relationship between the fraction of LAEs and redshift for $4 < z < 6$, and then extrapolating these trends to $z \sim 7$.

To determine the fraction of galaxies in our sample that belong to each absolute magnitude bin, we proceeded in the following way: for the galaxies with confirmed redshift, the absolute M_{UV} was derived from the observed Y-band magnitude and the spectroscopic redshift taking into account the effects of Lyα forest absorption at that redshift and the Lyα line flux contribution. They all have $M_{UV} < -20.25$. To assign an absolute magnitude M_{UV} to the remaining 14 galaxies with no spectroscopic confirmation, we proceeded in the following way. First, we randomly extracted a redshift from the $N(z)$ distribution function corresponding to our initial z-dropout selection (see C10a, Figure 1). From this random redshift and the observed Y-band magnitude, we derived M_{UV}. We repeated this procedure 10,000 times for each object and from the obtained M_{UV} distribution, we computed the fraction of galaxies in the two bins $-21.75 < M_{UV} < -20.25$ and $-20.25 < M_{UV} < -18.75$. In Figure 3 (upper panel), we plot as asterisks the fraction f of galaxies in the high-luminosity bin with EW > 55 Å ($F = 0.066$) and with EW > 25 Å ($F = 0.132$). In the lower

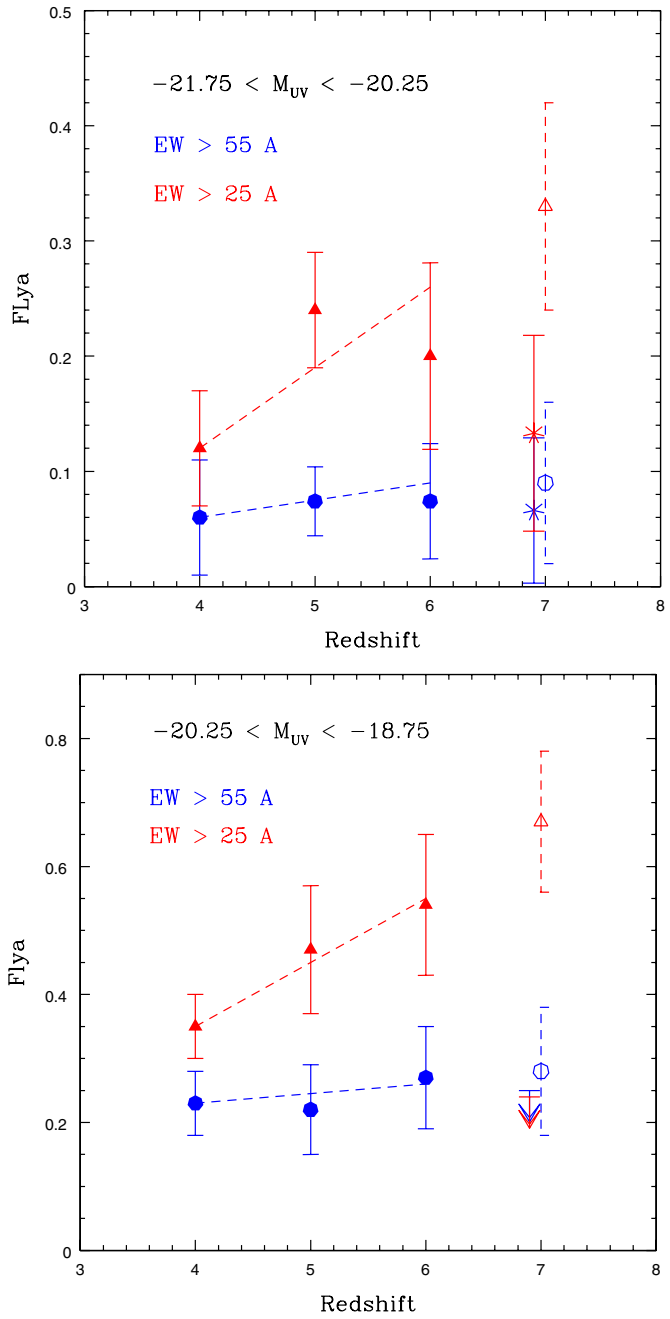

Figure 3. Upper panel: the fraction of LBGs with $-21.75 < M_{\rm UV} < -20.25$ showing Lyα emission at different redshifts and for different EW thresholds (25 Å in red and 55 Å in blue). The filled triangles and circles at $z \sim 4, 5$, and 6, respectively, are observations from S11; the open triangle/circle is their prediction for $z \sim 7$ on the basis of the fitted relation (dashed lines). The two asterisks are from this work. Lower panel: same as the upper panel for galaxies with absolute luminosity $-20.25 < M_{\rm UV} < -18.75$. The upper limits are from this work.

(A color version of this figure is available in the online journal.)

panel, we plot as limits the corresponding fraction for the low-luminosity galaxies, where we have no detections. Our points at $z \sim 6.9$ for the galaxies with EW > 25 Å are systematically below the expectations derived from S11 for $z \sim 7$ and are also lower than the observed fractions at $z \sim 6$. We are "missing" a consistent number of objects that should show Lyα with intermediate EWs (between 25 Å and 55 Å), while the fraction of galaxies with very bright Lyα emission (EW > 55 Å) is consistent with the predictions. Note that this is not due to a sensitivity limitation of our observations: our EW detection limit is well below EW $= 25$ Å for the whole spectral range probed and all galaxies with a broadband Y-magnitude brighter than 26.6, as shown in Figure 1 in F10 where we plotted the 10σ limit of the rest-frame EW as a function of redshift achieved by our observations. As we mentioned in Section 2, the limiting flux of the BDF and NTT field spectra is exactly the same as for the spectra of the GOODS-South field presented in F10.

As a final caveat we point out that we are comparing results at $z \sim 7$ obtained from homogeneous observations (in terms of setup, integration time, and so on) of a complete sample of galaxies to results that Stark et al. (2011) derived from a compilation of very heterogeneous observations carried out on different samples. This could potentially introduce some bias, although it is unclear in what direction.

4.2. Assessing the Significance of the EW Evolution

Given the small size of the sample, we made several tests to estimate the significance of our result. We assume that the distribution of the Lyα intensity in galaxies as a function of their rest-frame continuum magnitude $M_{\rm UV}$ does not change significantly from $z = 4$–6 to $z = 7$. We employ the same simulations developed in F10 and extensively described in that paper: briefly, we assume that at EW > 0 Å the EW distribution is represented by a Gaussian centered on EW $= 0$ Å with an additional constant tail up to 150 Å, and at EW < 0 by a constant level down to some EW minimum value, and null below. We take the width of the Gaussian and the two tails to reproduce the results of V09 and S10 at different rest-frame magnitudes, dividing the sample in two luminosity bins ($20.5 > M_{\rm UV}$ and $20.5 < M_{\rm UV} < 19.5$) and adjusting the two tails to reproduce the fraction of galaxies with EW > 50 Å given by S10 (for more details see F10).

We then compute the probability of detecting N Lyα lines at a given S/N in our sample. For each object, we randomly extract a redshift from the C10a distribution, we compute the corresponding $M_{\rm UV}$ from the observed Y-band magnitude and then we randomly extract an EW from the corresponding distribution. At the corresponding wavelength the minimum detectable EW is determined from the limiting flux density of our observations, which was shown in Figure 1 of F10 and fully takes into account the presence of skylines, etc. If the EW is larger than the minimum detectable EW, we conclude that the object would be detected. We repeat this procedure 10,000 times and in the end we compute the probability of having three detections with S/N > 10 (or five detections with S/N > 6) as observed in our sample.

The results for S/N > 10 are presented in Figure 4. If we assume that all 14 undetected objects are bona fide $z \sim 7$ galaxies the probability of finding our result, given the input EW distribution, is extremely low, below 2%. Even if we consider a consistent number of interlopers, and randomly eliminate three or four objects among the undetected ones, the probability is still as low as 3%–6%. The lower probability values are found if we systematically eliminate the fainter objects from our sample, since according to the input distribution, they are expected show the brightest Lyα lines. Vice versa, eliminating all the bright objects, the probability of our results is slightly larger.

To reconcile our observations to the redshift 6 distribution, with a low but acceptable probability (say ~10%), we have to remove ~7 candidates from our sample, i.e., assume an interloper fraction of 40%. Note that if we assume different

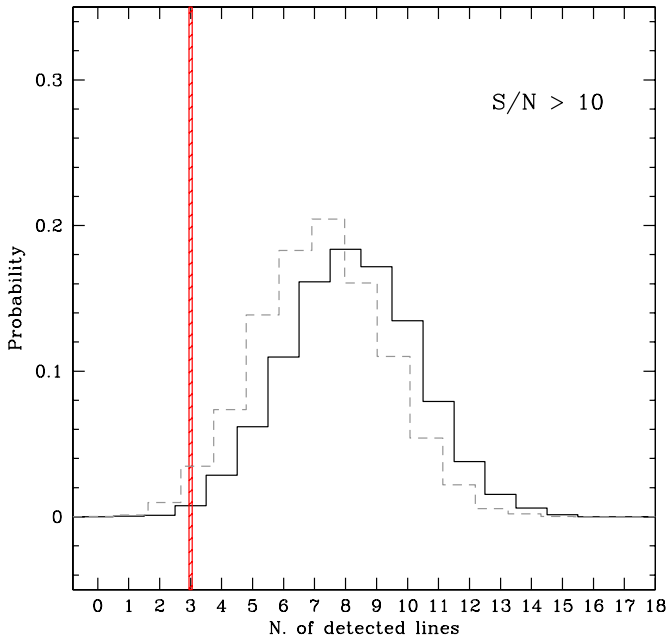

Figure 4. Probability distribution of the number of expected detections with S/N > 10 in our sample: black represents the case assuming no interlopers and gray assuming that the faintest three objects are interlopers. The red vertical region indicates the observed results: in both cases the probability of obtaining our results is very low (1%–3%).

(A color version of this figure is available in the online journal.)

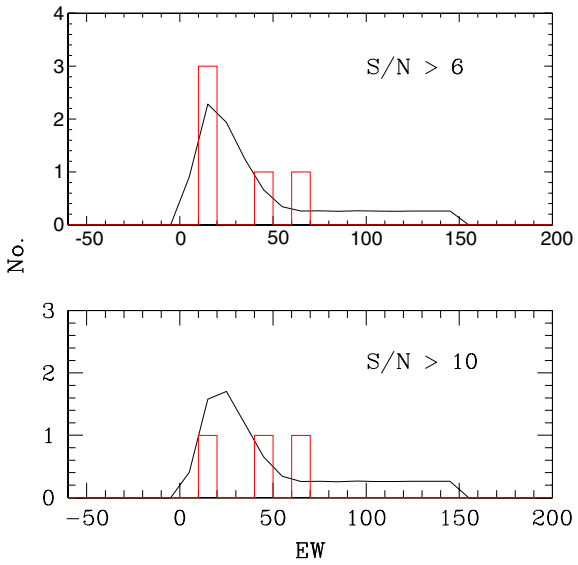

Figure 5. Black lines represent the expected EW distribution of our sample assuming that the 19 objects are at $z \sim 7$ and follow the same distribution as the S10 *i*-dropouts. The red histograms are the observed galaxies. The top panel is considering objects detected with S/N > 6 and the bottom panel for S/N > 10. The total number of objects expected is 9.7 in the first case (with 5 really observed) and 8.2 in the second (with 3 really observed).

(A color version of this figure is available in the online journal.)

EW distribution, such as the one from Stanway et al. (2007), our result is even less likely, due to a much higher tail of large EW objects in their sample which we do not observe.

Another way to visualize this result is by computing the expected distribution of EWs derived using the same simulations described above. The results are shown in Figure 5 for S/N = 6 and S/N = 10. In the first case, we expect 9.7 detections and we find 5. In the second case, we expect 8.2 detection and we have only 3. In both cases, it is clear that the number of expected detections is significantly higher than what we obtain and that, if the distribution of EW at $z = 7$ was the same as at $z = 6$, we should have detected more objects with intermediate EW (in the range 20–50 Å).

We conclude that the discrepancy between the expected EW distribution of z-dropout galaxies and the observed one is statistically significant. This confirms the results found in F10, with a sample that is three times as large.

5. INTERPRETING THE DROP OF LAE FRACTION AMONG LBGs: AN INCREASING NEUTRAL IGM ?

Our survey shows that there is a significant change in the fraction of LAEs among LBGs at $z > 6.5$: the trend for the fraction of Lyα emission in LBGs that is constantly increasing from $z \sim 3$ to $z \sim 6$ is stopped or most probably reversed at $z \sim 7$.

Evidence for a decrease in the fraction of bright Lyα emission in galaxies at redshift 6.5 and beyond was first claimed by Kashikawa et al. (2006), who noticed an apparent deficit at the bright end of the Lyα LF of LAEs, compared to that observed at $z = 5.7$. At even earlier epochs ($z \sim 7$), Ota et al. (2008) confirmed this significant decrease in LAE density with increasing redshift and interpreted it as due to a combination of galaxy evolution during these epochs and attenuation of the Lyα photons from LAEs by the neutral hydrogen possibly left at the last stage of cosmic reionization at $z \sim 6$–7. Subsequent searches for even higher redshift LAEs have all been unsuccessful so far (e.g., Clément et al. 2011; Hibon et al. 2010). However, the picture coming essentially from narrowband surveys for LAEs is still unclear, since other authors claimed instead that there is hardly any evolution in the density of LAEs at redshift beyond 7 (e.g., Tilvi et al. 2010) or that the evolution is only modest (Ouchi et al. 2010).

As already argued by other authors (e.g., F10; Ota et al. 2010), the drop in the frequency of bright Lyα lines in galaxies could be due to different effects (or a combination of them): (1) the LBG selection (z-dropouts) might suffer from an increasingly higher interloper fraction, such that a considerable number of our spectroscopic targets are not really at $z = 7$ but at much lower z; (2) there could be evolution in the intrinsic properties of the LBGs; and (3) an increasing neutral fraction of the IGM at $z > 6.5$ could suppress the Lyα emission.

We find it unlikely that a high fraction of interlopers is present in our sample for the following reasons: our deep spectroscopic observations of *i*-dropouts (see Section 3.2) show that the number of interlopers is actually rather modest, and that most of the objects that usually remain undetected in the spectroscopic surveys are actually at high redshift. We set a solid upper limit to the fraction of interlopers at $z = 6$ of $\leqslant$18%. The selection of z-dropouts is done along the same lines as the *i*-dropouts. Great care was put in excluding any possible interloper (see C10a for details) such that in the end we actually expect to have rejected a large number of real high-redshift galaxies from our sample, rather than include interlopers. For example, for the GOODS-South field we estimated, through detailed simulations, that our strict selection criteria reject about 30% of real high-z galaxies (C10a), and the fraction is similar or even higher for the other fields. Obviously, we cannot exclude the possibility that a population of unusual objects are contaminating our sample,

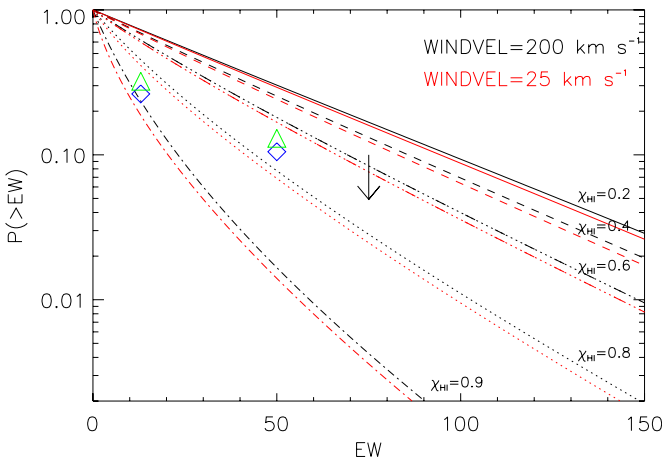

Figure 6. Expected cumulative distribution function of rest-frame EWs for $Z \sim 7$ LBGs, under the assumption that the observed LAE fraction at this redshift is different from $z \sim 6$ only because of the IGM. The different lines correspond to a universe that was, respectively, ∼0.2, 0.4, 0.6, 0.8, and 0.9 neutral by volume (from top to bottom). The black lines are for the wind model with $(N_{\rm H\,I}, v_{\rm wind}) = (10^{20}\,{\rm cm}^{-2}, 200\,{\rm km\,s}^{-1})$ while the red lines are for $(N_{\rm H\,I}, v_{\rm wind}) = (10^{20}\,{\rm cm}^{-2}, 25\,{\rm km\,s}^{-1})$. The blue diamonds (green triangles) are our results assuming that 0%(20%) or the undetected galaxies are interlopers. The upper limit for EW = 75 Å is from Stark et al. (2011).

(A color version of this figure is available in the online journal.)

but there is no reason why they should also not appear in the *i*-dropout spectroscopic sample.

Evolution in the intrinsic properties of the galaxies, such as an increasing dust content at higher redshift, could also provide an explanation for the missing Lyα. However, as we go to earlier cosmic epochs we expect to find still younger objects, more metal and dust poor: in this case the production of Lyα photons should be enhanced and we would expect to find an increasing fraction of Lyα emitting galaxies (e.g., Shimasaku et al. 2006). Indeed galaxies at very high redshift tend to show steep UV slopes (e.g., V11; Bouwens et al. 2010b), consistent with the hypothesis that these are relatively dust free systems.

Alternatively, a very high escape fraction of ionizing photons in high z-galaxies could also reduce the intrinsic Lyα emission (e.g., Dayal et al. 2008). The evolution of the escape fraction at high redshift is unknown at present (e.g., Haardt & Madau 2011; Boutsia et al. 2011, and references therein). Furthermore for relatively high IGM neutral gas fraction, the Lyα luminosity does not depend on $f_{\rm esc}$ in a monotonic way (Dayal et al. 2008), since the effect of $f_{\rm esc}$ is not only on the intrinsic Lyα line but also on the Strömgren sphere size and hence on the visibility of the line itself (see also Santos 2004). For clarity we point out that both Santos (2004) and Dayal et al. (2008) are examples of homogeneous reionization models, in which the galaxy creates its own H II region. This introduces a direct relation between a galaxy's intrinsic luminosity and it is the H II bubble size. In more realistic inhomogeneous reionization models, the H II bubble size is determined mostly by lower mass halos, which host less luminous galaxies. Hence the effects of a higher $f_{\rm esc}$ on the Lyα visibility are less certain.

Here we therefore attempt to interpret the apparent fast drop in the LAE fraction among LBGs in terms of an evolving neutral hydrogen fraction. For this we employ the models developed by Dijkstra & Wyithe (2010), which combine galactic outflow models with large-scale semi-numeric simulations of reionization to quantify the probability distribution function of the fraction of Lyα photons transmitted through the IGM $\mathcal{T}_{\rm IGM}$.

Dijkstra et al. (2011) derive the $\mathcal{T}_{\rm IGM}$ by extracting $\sim 10^4$ lines of sight centered on halos in the mass range, $10^{10}\,M_\odot < M_{\rm halo} < 3 \times 10^{10}\,M_\odot$. This choice of host halo masses was motivated by the UV-derived SFR of few (2–4) $M_\odot\,{\rm yr}^{-1}$ of the candidate $z = 8.6$ galaxy by Lehnert et al. (2010), which corresponds to a halo mass of $>10^{10}\,M_\odot$ in the cosmological hydrodynamic simulations of Trac & Cen (2007). Our galaxies have similar or brighter UV luminosities than this object, therefore we assume they are hosted by halo of similar or higher masses.

In Dijkstra et al. (2011), the observed EW-distribution function at $z \sim 6$ is modeled as an exponential function which provides a good fit to the observed one at lower redshifts (e.g., Gronwall et al. 2007), with a scale length that corresponds to the median value observed by Stark et al. (2010) of 50 Å. The IGM at redshift 6 is assumed 100% transparent to Lyα photons emitted by galaxies: the EW probability distribution function at $z = 7$ is different from that at $z = 6$ only because of evolution of the ionization state of the IGM. The simulations assume no dust.

This exercise is repeated for various fractions of neutral hydrogen (by volume), $\chi_{\rm H\,I} = 0.21, 0.41, 0.60, 0.80, 0.91$. The results are shown in Figure 6 for two models that differ only for the velocity of the outflowing winds assumed (25 and 200 km s^{-1}) and have the same column density $N_{\rm H\,I} = 10^{20}\,{\rm cm}^{-2}$. In the case of higher velocity (black lines), the transmitted fraction of Lyα radiation increases; the same is true if the column density is increased.

Our observations (blue diamonds) are consistent with a neutral hydrogen fraction larger than $\chi_{\rm H\,I} = 0.60$, even assuming that among the 14 undetections the fraction of interlopers is as high as 20% (green triangles). This latter value was chosen assuming the percentage of interlopers at $z \sim 7$ is equal to the upper limit we derived at $z \sim 6$. In the same figure, we also indicate the upper limit derived by Stark et al. (2011) from their undetections at $z = 7$, given their sensitivity to EW > 75 Å. Clearly, there are many assumptions in the models, not least the fact that the universe is considered completely reionized at $z = 6$.

For a comparison, Ota et al. obtained an estimate of $\chi_{\rm H\,I}^{z=7} \sim 0.32$–$0.62$ from the lack of LAEs in the deep NB973 survey of the Subaru Deep Field (Ota et al. 2008, 2010) and using the Santos (2004) reionization models. Also, spectral analysis of $z \sim 6.3$ and 6.7 gamma-ray bursts implies that reionization is not yet complete at these epochs with $\chi_{\rm H\,I}^{z=6.3} \leqslant 0.17$–$0.6$ (Totani et al. 2006; but see also McQuinn et al. 2008 for a different analysis) and $\chi_{\rm H\,I}^{z=6.7} > 0.35$ (Greiner et al. 2009). Finally, the recent observations of the most distant QSO known at $z = 7.08$ (Mortlock et al. 2011) were analyzed by Bolton et al. (2011), who showed that the transmission profile is consistent with an IGM in the vicinity of the quasar with a volume averaged H I fraction of $\chi_{\rm H\,I} > 0.1$.

Overall these results, together with the high neutral fraction that we derive, point to a rapid evolution of the neutral fraction of hydrogen in the universe between $z \sim 6$ and $z \sim 7$, in required of the order of $\Delta\chi_{\rm H\,I} \sim 0.6$ in a short time ($\Delta z = 1$).

6. SUMMARY AND CONCLUSIONS

We have presented and discussed spectroscopic observations of a sample of 20 z-dropout galaxies selected from our deep and wide Hawk-I imaging program (C10a; C10b). We confirm the redshifts of five galaxies at $6.6 < z < 7.1$, through the presence of an Lyα emission line. Only two of these galaxies have bright

Lyα and relatively high EWs. The number of galaxies detected in our survey is considerably smaller than what is expected from lower redshift surveys: the trend for an increasing fraction of Lyα emission in LBGs that was found to hold from redshift 3 to 6 by previous studies (S11) is halted and most probably reverted from $z = 6$ to $z = 7$.

If we assume that the intrinsic EW distribution of Lyα is the same at $z \sim 7$ as has been observed at $z \sim 6$, the discrepancy between the predicted and measured EW distributions in our z-dropout sample is statistically significant. Our result would be marginally consistent with no evolution only if as many as half of the unconfirmed galaxies were interlopers. The required interloper fraction would be much larger than what we observe in our sample of i-dropouts, where interlopers are less than or equal to 18%, as well as what is commonly found in lower redshift samples (e.g., S10; V09).

These results extend and confirm those of F10, with a sample that is almost three times larger. The very recent works presented by Ono et al. (2011) and Schenker et al. (2011) on LBG samples that are largely complementary to ours in terms of $M_{\rm UV}$ are also in agreement with our results.

The low detection rate and the modest EW found can be explained in terms of a rapid evolution of the neutral hydrogen fraction from $z \sim 6$ to $z \sim 7$. Assuming that the universe was completely reionized at $z = 6$, our result points are consistent with a change of neutral hydrogen of the order of $\Delta\chi_{\rm H\,I} \sim 0.6$ in a relatively short time $\Delta z \sim 1$. Indeed, there is no evidence at all that the universe is completely ionized at $z = 6$, e.g., Mesinger (2010) argues that, since reionization is expected to be highly inhomogeneous, much of the spectra pass through just the ionized component of the IGM even for non-negligible values of neutral hydrogen fraction (volume mean; see also McGreer et al. 2011). However, if we want to lower substantially the $\Delta\chi_{\rm H\,I}$ implied by our observations, then we need the universe at $z = 6$ to be substantially neutral (>10%).

In any case, even if the model uncertainties are large, the absence of strong Lyα emission lines in our high-redshift galaxies is very striking, and together with the very low number of LAEs found in all recent deep narrowband surveys at $z \geqslant 7$ points to some drastic change that took place around that redshift. To better quantify the increase in the hydrogen neutral fraction at these epochs in the near future we will exploit the deep multi-wavelength CANDELS data set (Grogin et al. 2011; Koekemoer et al. 2011), which will provide large numbers of candidate $z \sim 7$ galaxies for further spectroscopic follow-up campaigns.

We acknowledge the support of ASI-INAF in the framework of the program I/009/10/0 supporting Data Analysis in the field of Cosmology. Observations were carried out using the Very Large Telescope at the ESO Paranal Observatory under Programme IDs 084.A-095, 085.A-0844, 283.A-5052, and 181.A-0717.

REFERENCES

Arnouts, S., D'Odorico, S., Cristiani, S., et al. 1999, A&A, 341, 641
Bolton, J. S., Haehnelt, M. G., Warren, S. J., et al. 2011, MNRAS, 416, L70
Boutsia, K., Grazian, A., Giallongo, E., et al. 2011, ApJ, 736, 41
Bouwens, R. J., Illingworth, G. D., Oesch, P. A., et al. 2010a, ApJ, 709, L133
Bouwens, R. J., Illingworth, G. D., Oesch, P. A., et al. 2010b, ApJ, 708, L69
Bunker, A. J., Stanway, E. R., Ellis, R. S., McMahon, R. G., & McCarthy, P. J. 2003, MNRAS, 342, L47
Castellano, M., Fontana, A., Boutsia, K., et al. 2010a, A&A, 511, A20 (C10a)
Castellano, M., Fontana, A., Paris, D., et al. 2010b, A&A, 524, A28 (C10b)
Clément, B., Cuby, J. -G., Courbin, F., et al. 2011, arXiv:1105.4235
Dayal, P., Ferrara, A., & Gallerani, S. 2008, MNRAS, 389, 1683
Dayal, P., Maselli, A., & Ferrara, A. 2011, MNRAS, 410, 830
Dijkstra, M., Mesinger, A., & Wyithe, J. S. B. 2011, MNRAS, 414, 2139
Dijkstra, M., & Wyithe, J. S. B. 2010, MNRAS, 408, 352
Dow-Hygelund, C. C., Holden, B. P., Bouwens, R. J., et al. 2007, ApJ, 660, 47
Dunlop, J. S., McLure, R. J., Robertson, B. E., et al. 2011, arXiv:1102.5005
Finkelstein, S. L., Papovich, C., Giavalisco, M., et al. 2010, ApJ, 719, 1250
Fontana, A., D'Odorico, S., Poli, F., et al. 2000, AJ, 120, 2206
Fontana, A., Vanzella, E., Pentericci, L., et al. 2010, ApJ, 725, L205
Giavalisco, M., Ferguson, H. C., Koekemoer, A. M., et al. 2004, ApJ, 600, L93
Grazian, A., Castellano, M., Koekemoer, A. M., et al. 2011, A&A, 532, A33
Greiner, J., Krühler, T., Fynbo, J. P. U., et al. 2009, ApJ, 693, 1610
Grogin, N. A., Kocevski, D. D., Faber, S. M., et al. 2011, arXiv:1105.3753
Gronwall, C., Ciardullo, R., Hickey, T., et al. 2007, ApJ, 667, 79
Haardt, F., & Madau, P. 2011, arXiv:1105.2039
Hibon, P., Cuby, J.-G., Willis, J., et al. 2010, A&A, 515, A97
Kashikawa, N., Shimasaku, K., Malkan, M. A., et al. 2006, ApJ, 648, 7
Koekemoer, A. M., Faber, S. M., Ferguson, H. C., et al. 2011, arXiv:1105.3754
Labbé, I., Gonzlez, V., Bouwens, R. J., et al. 2010, ApJ, 716, L103
Lehnert, M. D., & Bremer, M. 2003, ApJ, 593, 630
Lehnert, M. D., Nesvadba, N. P. H., Cuby, J.-G., et al. 2010, Nature, 467, 940
McGreer, I. D., Mesinger, A., & Fan, X. 2011, MNRAS, 415, 3237
McLure, R. J., Dunlop, J. S., Cirasuolo, M., et al. 2010, MNRAS, 403, 960
McQuinn, M., Lidz, A., Zaldarriaga, M., Hernquist, L., & Dutta, S. 2008, MNRAS, 388, 1101
Mesinger, A. 2010, MNRAS, 407, 1328
Mortlock, D. J., Warren, S. J., Venemans, B. P., et al. 2011, Nature, 474, 616
Oesch, P. A., Bouwens, R. J., Illingworth, G. D., et al. 2010, ApJ, 709, L16
Ono, Y., Ouchi, M., Mobasher, B., et al. 2011, arXiv:1107.3159
Ota, K., Iye, M., Kashikawa, N., et al. 2008, ApJ, 677, 12
Ota, K., Iye, M., Kashikawa, N., et al. 2010, ApJ, 722, 803
Ouchi, M., Mobasher, B., Shimasaku, K., et al. 2009, ApJ, 706, 1136
Ouchi, M., Shimasaku, K., Furusawa, H., et al. 2010, ApJ, 723, 869
Robertson, B. E., & Ellis, R. S. 2011, arXiv:1109.0990
Santos, M. R. 2004, MNRAS, 349, 1137
Schenker, M. A., Stark, D. P, Ellis, R. S., et al. 2011, arXiv:1107.1261
Shimasaku, K., Kashikawa, N., Doi, M., et al. 2006, PASJ, 58, 313
Stanway, E. R., Bunker, A. J., Glazebrook, K., et al. 2007, MNRAS, 376, 727 (S07)
Stanway, E. R., Bunker, A. J., McMahon, R. G., et al. 2004, ApJ, 607, 704
Stark, D. P., Ellis, R. S., Chiu, K., Ouchi, M., & Bunker, A. 2010, MNRAS, 408, 1628
Stark, D. P., Ellis, R. S., & Ouchi, M. 2011, ApJ, 728, L2
Tilvi, V., Rhoads, J. E., Hibon, P., et al. 2010, ApJ, 721, 1853
Totani, T., Kawai, N., Kosugi, G., et al. 2006, PASJ, 58, 485
Trac, H., & Cen, R. 2007, ApJ, 671, 1
Vanzella, E., Giavalisco, M., Dickinson, M., et al. 2009, ApJ, 695, 1163
Vanzella, E., Pentericci, L., Fontana, A., et al. 2011, ApJ, 730, L35
Wilkins, S. M., Bunker, A. J., Ellis, R. S., et al. 2010, MNRAS, 403, 938